[1]Hamad Alharkan

Robust H-Infinity Speed Controller based Optimization Technique for Doubly Salient Singly Excited Motor Drive

Journal of Electrical Systems

Abstract: - This research presents a novel robust H_∞ controller for Doubly Salient Singly Excited motor (DSSEM) speed controlling. This algorithm aims to minimize the influence of disturbances that affect motor function and offer the best duty cycles possible to accomplish tracking performance. The H-infinity (H_∞) tracking control approach can optimally solve the tracking game algebraic Riccati equation online by using reinforcement learning. This method enhances the Doubly Salient Singly Excited Motor (DSSEM) system model with the reference current model to produce a quadratic value function. The quadratic value function facilitates the implementation of a linear quadratic tracker, similar to H_∞ control. By partitioning and organizing the nonlinear domain of the DSSEM into a table of H_∞ nodes, the system can manage complex nonlinearities efficiently. Each H_∞ node in the table represents a specific region of the control space, allowing for precise and robust tracking of desired reference signals. This structure ensures that the DSSEM achieves optimal performance and stability, adapting dynamically to operational changes. Furthermore, the H_∞ tracking control is outfitted with a linear interpolation method to facilitate a seamless transition between H_∞ matrices in the table. Finally, this paper presents simulation results to validate the proposed control algorithm.

Keywords: Doubly Salient Singly Excited motor (DSSEM), Speed control, Reinforcement learning (RL), Optimization problems, Machine learning method.

I. INTRODUCTION

Recently, Doubly Salient Singly Excited motors, or DSSEMs, have drawn much interest for their high-performance uses in electric cars and airplanes, among other high-performance applications. [1]–[5]. The reported rise in DSSEM use in commercial and industrial applications is dependent on various factors, including fault-tolerant capability, a fault-tolerant design that eliminates the need for a magnet or rotor winding, low cost as a result of the decline in semiconductor switch prices, and high speed and high-efficiency capabilities [6], [7]. Additionally, the rising usage of DSSEM in various applications has been spurred by the global trend to limit the use of magnets, advanced technology in electronic devices, and capacitors to regulate pulse-type current motors. On the other hand, the high nonlinearity of DSSEM presents a significant problem in many applications, leading to a large ripple in the generated torque. A significant electromechanical variation based on the phase current fluctuation and the rotor movement is exhibited by DSSEMs because of their prominent structure and enormous saturation. This may cause vibration, noise, and harness during machine operations. Consequently, the undesired torque ripple must be removed to improve the machine's performance.

Optimizing the machine's dynamic performance mostly depends on the DSSEM drive's present controller. A major responsibility of the machine's speed controller is to provide an accurate current pulse and high bandwidth that the controller may utilize to track the correct current trajectory [8]. However, internal motor disturbances, such as the reverse electromotive force (EMF) produced by flowing an erratic current through the stator winding, affect how well the current schemes work. In order to solve this problem, the motor should be given a comparatively high DC voltage injection, which will cause the current to rise and fall very quickly. It is imperative to employ a highly dependable current controller with extensive modulation and control frequency handling to achieve this performance level. A thorough investigation into existing control has been conducted to enhance DSSEM performance [9]–[22]. Delta modulation, which has an upper cap for the switching frequency and hence a significant torque ripple, is a popular technique for modulating the current in the DSSEM drive [10], [11]. DSSEM has made use of the Proportional-Integral (PI) current controller [9], [12]. Due to its slowness and inability to pick controller parameters that can handle all operating situations, the PI dynamic, in this instance, is unsuitable to generate the intended current pulse. To regulate the speed while lessen current ripples, researchers have looked into cutting-edge intelligent strategies like artificial neural networks, model predictive control (MPC), and neuro-fuzzy controllers (NFC) [16]–[20]. As an adaptive dynamic programming technique that can handle both tracking control and adaptation at the same time, [21], [22] presented a Q-learning scheduling controller in contrast to previous

[1] Department of Electrical Engineering, College of Engineering, Qassim University, Buraydah 52571, Saudi Arabia;
*Correspondence: h.alhrkan@qu.edu.sa

approaches that call for a separate approximator to approximate the value of inductance with respect to current and rotor angle. In [22], the tracking problem is solved using the optimal algorithm, which is based on the reinforcement learning technique. In order to create a controller that can track the reference path, the Q-learning algorithm produced the cost function of the infinite-horizon linear quadratic tracker (LQT). The algorithm's synthesis relies on linear modeling and is limited to local applications inside the nonlinear domain, such as DSSEM. By scheduling linear Q-controllers across the nonlinear DSSEM surface, a linear parameters variable gain scheduling approach has been introduced to ensure the execution of nonlinear control, substantially extending the linear model to match the nonlinear system. In order to achieve this goal, [22] suggested a collection of Q-cores mounted on the DSSEM inductance profile. Each Q-core is positioned at a locally linearized region where the Q-learning algorithm can be run. In order to apply the scheduling mechanism, data gathered during machine operation was used to train a readout table of Q matrices, which is used in this paper to construct H_∞ matrices instead of Q matrices. The primary problem with the Q-learning controller, despite the algorithm's good tracking performance, is that the control scheme does not consider the disturbances as being minimized under operation conditions.

In this study, a robust switching H_∞ control was added to control the speed by solving the tracking game algebraic Riccati equation (GARE), and then, to solve the two-player zero-sum issue [23]. Phase voltage is one player in this game, which aims to minimize the value function. On the other hand, the disturbance input, which aims to maximize the value function, is the other player. Based on the linear model, the H_∞ method is also generated; DSSEM has a large amount of fluctuation in inductances depending on stator current and rotor position. Therefore, to smoothly switch between the learned H_∞ matrices positioned on the trajectory of the system's states when the speed is changed, a trilinear interpolation approach based on a grid of H_∞ controllers for a selective local point has been presented. This work introduces a robust nonlinear speed controller for DSSEM drives that minimizes torque ripples while achieving optimal and adaptive performance.

This paper's primary contributions include: i) introducing H_∞ tracking control for DSSEM, ii) presenting a matrices of H_∞ nodes that characterize DSSEM's nonlinearity, and iii) suggesting a trilinear interpolation method for a precise transition between H_∞ nodes in the system's state.

II. H_∞ Control for Zero-sum Game Problem of DSSEM

Linear quadratic tracker (LQT) has become an increasingly vital design tool for tracking controls. Obtaining the optimal LQT solution enables tracking a predetermined reference signal by minimizing the cost function and the difference between the reference and output currents [19]. Typically, LQT solutions were derived by independently acquiring the solutions for the feedforward and feedback sections. The primary disadvantage of the solution is that it was computed offline in conjunction with the model's parameters [19]. In this context, the Reinforcement Q-learning technique, which is a type of adaptive dynamic programming, provides an online solution to LQT problems without using DSSEM model information. This section presents the derivation of the LQT-augmented system. Additionally, the optimal solutions for LQT utilizing the Bellman equation and Q-learning are included.

H_∞ is a robust controller that can be incorporated with adaptive tracking control to minimize the impact of disturbances of DSSEM and to verify if the output current follows the reference current. Traditionally, the H_∞ tracking control problem has been solved using the linear matrix inequality (LMI) approach [24], [25]. Due to the difficulty of processing LMI, this method requires a significant computational load to tackle the issue, which is impractical for some industrial applications. The primary benefit of H_∞ tracking control for DSSEM applications is its application in zero-sum game problems and its execution through RL techniques. In this game, disruption maximizes the cost function while the controller minimizes it. A unique solution where the saddle point of the control input and disturbance can be reached using the H_∞ tracking control. [26], [27]. This procedure can be implemented by determining the GARE's optimal solution [28]. The optimal control problem can be resolved using adaptive dynamic programming, which incorporates reinforcement learning algorithms, dynamic programming techniques, and adaptive cretic [29]–[31]. In this study, a subfield of machine learning theory called reinforcement learning used machine feedback data to enhance system behavior. In order to complete this process, the augmented model of the machine used the RL methods' predefined reference of the periodic waveform model to build a discounted quadratic value function for the H_∞ tracking problem [32]. When the value function was quadratic, the zero-game problem was resolved by developing the Bellman equation. GARE was derived and applied to the H_∞ tracking problem using the DSSEM augmented model. Then, the GARE was solved to allow the controller's feedforward and feedback terms to find optimal solutions simultaneously [26].

This study aimed to resolve the H_∞ tracking issue by designing the Bellman equation applying the policy iteration approach. This section introduces the formulation of the H_∞ tracking control, the generation of the zero-sum games issue, and the use of the RL approach to design the tracking control of DSSEM.

A. Formulating the DSSEM Model for H_∞ Tracking Control

The assumption used for many DSSEM structures in the literature serves as the basis for generating the DSSEM model. The mutual inductances between neighboring coils in the stator were ignored. Considering this assumption and the presence of the disturbance, the discrete-time domain of the DSSEM model based on the forward technique were characterized as follows:

$$x_{k+1} = (1 - TR/L_k)x_k + (T/L_k)u_k + Dw_k \tag{1}$$

The phase current was denoted by x_k, the applied DC voltage by u_k, the phase resistance by R, the disturbance input by w_k, and the dynamic disturbance matrix by D. L_k was the nonlinear phase inductance with respect to the rotor angle and phase current, while T was the sample time. Developing an algorithm to confirm that the phase current x_k of DSSEM can optimally trace the reference current r_k, was the primary goal of H_∞ tracking control. Therefore, it became possible to ascertain the tracking error of the issue as $e_k = x_k - r_k$. Next, the tracking error and phase voltage were used to determine the performance index, which can then be given as:

$$\|s_k\|^2 = (x_k - r_k)^T Q(x_k - r_k) + u_k^T R u_k \tag{2}$$

where Q and R represented the operator-predefined positive weight matrices for the phase voltage and tracking error, respectively. The DSSEM model (1) was linearized to obtain the L2-gain condition needed to create a H_∞ tracking control. L2-gain has to be equivalent to or less than γ if:

$$\sum_{k=0}^{\infty} \|s_k\|^2 \le \gamma^2 \sum_{k=0}^{\infty} \|w_k\|^2 \tag{3}$$

For all $w_k \in L_2[0, \infty)$, where $\gamma \ge 0$ was the disturbance attenuation preset value. The disturbance attenuation condition, or equation (3), lessened the effects of the disturbance input to the machine by the value of γ. Therefore, the H_∞ tracking algorithm aimed to provide a phase voltage that satisfied equation (3) and maintained system stability when the disturbance input dropped to zero. The infinite-horizon H_∞ tracking control's performance index function was expressed as follows based on equation (3):

$$J(x_k, r_k, u_k, w_k) = \sum_{i=k}^{\infty} U_i = \sum_{i=k}^{\infty} [(x_i - r_i)^T Q(x_i - r_i) + u_i^T R u_i - \gamma^2 w_i^T w_i] \tag{4}$$

where the utility function was represented by U. It should be noted that the tracking error and the DSSEM model's phase voltage signals was penalized by using the matrices of Q and R as design parameters. Utilizing the value function based on the DSSEM augmented model given acceptable control and disturbance input was formulated as follows:

$$V(x_k, r_k) = J(x_k, r_k, u_k, w_k) \tag{5}$$

The augmented model for the H_∞ tracking controller was then designed by assuming that the reference current of DSSEM was produced by the reference current model, which offered a variety of current trajectories [32]. The following equation provided the waveform of the reference current:

$$r_{k+1} = Fr_k \tag{6}$$

where $F \in \mathbb{R}^n$ is the reward of generating a certain current path. Currently, the reference current model (6) and the DSSEM model (1) was used to provide the augmented model as:

$$X_{k+1} = A_a X_k + B_b u_k + D_d w_k \tag{7}$$

where $A_a = \begin{bmatrix} 1 - TR/L_k & 0 \\ 0 & F \end{bmatrix}$, $B_b = \begin{bmatrix} (T/L_k) \\ 0 \end{bmatrix}$, and $D_d = \begin{bmatrix} D \\ 0 \end{bmatrix}$. The augmented state, which included the output current and the reference current trajectory, was generated as $X_k = [x_k^T \quad r_k^T]^T$ based on the augmented model (7). It is important to note that the value function (5) was only implemented if F is Hurwitz with respect to the reference current model (6). In order to resolve this problem, the discounted value function of the

H_∞ tracking control based on the DSSEM (7) augmented model was introduced as:

$$V(X_k) = \sum_{i=k}^{\infty} \lambda^{i-k} \left[X_i^T Q_q X_i + u_i^T R u_i - \gamma^2 w_i^T w_i\right] \tag{8}$$

where $Q_q = [I \quad -I]^T Q [I \quad -I]$, and $0 < \lambda \leq 1$ is a discount factor. Therefore, the condition of disturbance attenuation was created as:

$$\sum_{i=0}^{\infty} \lambda^i \left[X_i^T Q_q X_i + u_i^T R u_i\right] \leq \gamma^2 \sum_{i=0}^{\infty} \lambda^i \, w_i^T w_i \tag{9}$$

B. Designing Tracking Control for formulating the Zero-Sum Game equation

The H_∞ tracking problem based on two-player zero-sum (ZS) games is described in this section. Phase voltage was one player in this game, which aimed to minimize the value function. The disturbance input, on the other hand, was the other player and aimed to maximize the value function. The goal of the ZS games problem was to find the only solution that satisfied the feedback optimal solutions for the disturbance input and the control input, as expressed in the equation below:

$$V^*(X_k) = \min_{u_k} \max_{w_k} \sum_{i=k}^{\infty} \lambda^{i-k} \left[X_i^T Q_q X_i + u_i^T R u_i - \gamma^2 w_i^T w_i\right] \tag{10}$$

The Bellman equation was produced using the Bellman optimization approach for the value function.

$$V(X_k) = X_k^T Q_q X_k + u_k^T R u_k - \gamma^2 w_k^T w_k + \lambda V(X_{k+1}) \tag{11}$$

The value function's quadratic version, $V(X_k) = X_k^T H X_k$, was validated [32]. Thus, it became possible to rewrite the value function as:

$$X_k^T H X_k = X_k^T Q_q X_k + u_k^T R u_k - \gamma^2 w_k^T w_k + \lambda X_{k+1}^T H X_{k+1} \tag{12}$$

The tracking problem's Hamiltonian function was generated as follows in order to define the saddle points for the phase voltage and the disturbance policy:

$$(X_k, u_k, w_k) = X_k^T Q_q X_k + u_k^T R u_k - \gamma^2 w_k^T w_k + \lambda X_{k+1}^T H X_{k+1} - X_k^T H X_k \tag{13}$$

The ideal phase voltage u_i^* stationary state and the worst-case disturbance input w_i^* was attained as $\partial h(X_k, u_k, w_k)/\partial u_k = 0$ and $\partial h(X_k, u_k, w_k)/\partial w_k = 0$, respectively [26]. Hence, the following equations were generated:

$$u_k^* = -K^* X_k \tag{14}$$

$$w_k^* = -S^* X_k \tag{15}$$

Where

$$K^* = [R + \lambda B_b^T H B_b + \lambda^2 B_b^T H D_d (\gamma^2 I - \lambda D_d^T H D_d)^{-1} D_d^T H B_b]^{-1} \times [\lambda B_b^T H A_a + \lambda^2 B_b^T H D_d (\gamma^2 I - \lambda D_d^T H D_d)^{-1} D_d^T H A_a] \tag{16}$$

$$S^* = [\lambda D_d^T H D_d - \gamma^2 I - \lambda^2 D_d^T H B_b (R + \lambda B_b^T H B_b)^{-1} B_b^T H D_d]^{-1} \times [\lambda D_d^T H A_a + \lambda^2 D_d^T H B_b (R + \lambda B_b^T H B_b)^{-1} B_b^T H A_a] \tag{17}$$

After substituting (16) and (17) into (13) and rearranging a few times, the parameters of the H matrix were obtained, leading to the optimal GAME solution for the H_∞ tracking issue.

$$H = Q_q + \lambda A_a^T P A_a - \lambda^2 [A_a^T P B_b \quad A_a^T P D_d] \times \begin{bmatrix} R + \lambda B_b^T H B_b & \lambda B_b^T H D_d \\ \lambda D_d^T H B_b & \lambda D_d^T H D_d - \gamma^2 I \end{bmatrix}^{-1} \begin{bmatrix} B_b^T H A_a \\ D_d^T H A_a \end{bmatrix} \tag{18}$$

Therefore, the SZ game issue given in (10) was solved by the equations (14) to (18), which also guaranteed the achievement of the disturbance attenuation condition given in (9) [26].

C. Adopting the Reinforcement Learning Algorithm for Solving Tracking Problem on-line

This section describes the development and application of the RL-based policy iteration (PI) algorithm to determine the best way to track GARE online [33]. Recursively using data packets collected during machine operation, the value function, control law, and disturbance policy were changed. The Bellman equation was utilized

to solve the problem, and the results obtained were the two model-based PI methods. Zero sum game problem based reinforcement learning Algorithm which can solve the online tracking problem is illustrated in Fig 2.

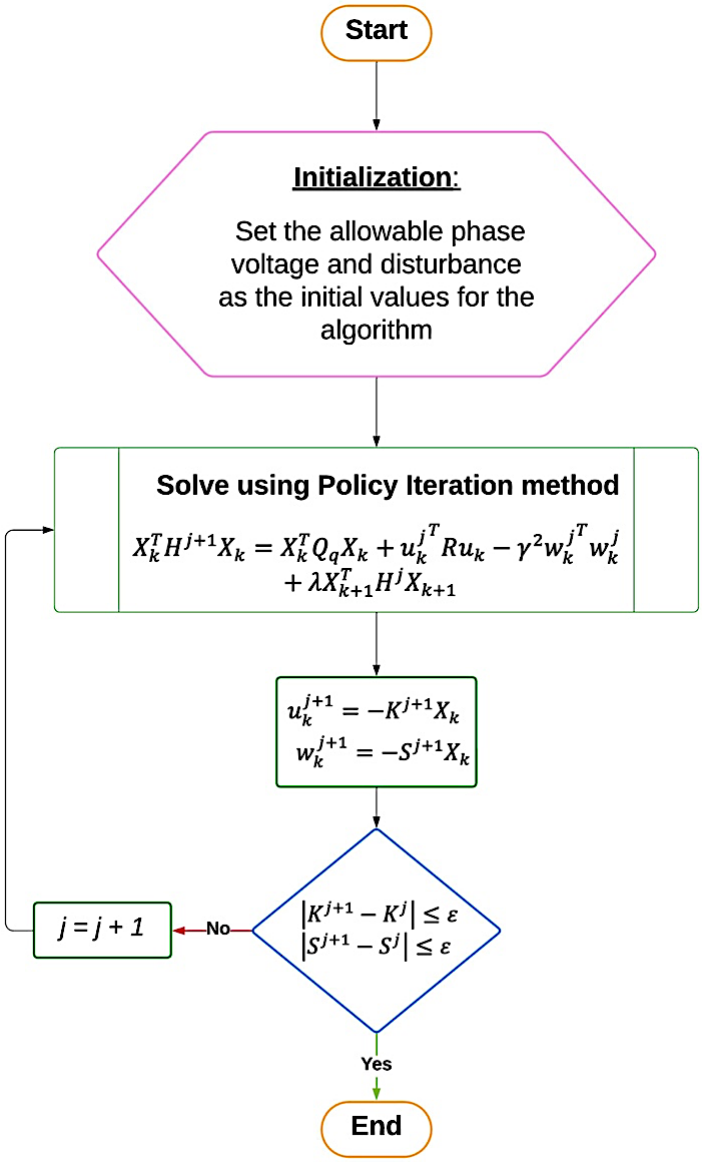

Fig 2. Flowchart of zero-sum game reinforcement learning.

III. A TRILINEAR ESTIMATION ALGORITHM FOR CONTROLLING THE SPEED OF DSSEM

Doubly Salient Singly Excited motors (DSSEMs) are a unique class of electric machines characterized by a distinct construction where the stator and rotor have varying numbers of poles. This design leads to an intriguing dynamic where the movement of the rotor induces fluctuations in the reluctance of the magnetic flux within the motor. When the stator and rotor are perfectly aligned, the reluctance of the magnetic circuit is minimized, resulting in maximum inductance in the motor's inductance-profile. This configuration is ideal for efficient energy conversion. Conversely, when the alignment between the stator and rotor is completely misaligned, the reluctance of the magnetic circuit is maximized, leading to minimal inductance. Achieving effective electromechanical energy conversion in DSSEMs requires designing them to operate under high levels of magnetic saturation. This characteristic enables the motor to efficiently handle varying loads and operating conditions. The inductance per phase in an DSSEM can vary with the current flowing through it. This variation is primarily attributed to the changing magnetic properties resulting from the different alignments of the stator and rotor. When the stator and rotor are aligned, the inductance experiences significant changes with varying current levels, mainly due to the narrow air gap between them. On the other hand, when the stator and rotor are misaligned, the larger air gap results in only slight variations in inductance. In theory, the inductance profile of an DSSEM exhibits trapezoidal waveforms due to the idealized behavior of the magnetic circuit. However, in practical applications, factors such

as magnetic saturation lead to rounded corners in the waveform, resulting in sinusoidal shapes with slightly varying frequencies. The inductance profile of an actual DSSEM, such as a 12/8 configuration, depends on both the current flowing through it and the position of the rotor. This dependence is illustrated in Fig 1, where the inductance varies with different current levels and rotor positions, providing insight into the motor's performance characteristics under various operating conditions. Traditional controllers for managing the speed of Doubly Salient Singly Excited motor (DSSEM) drives, like the hysteresis controller, offer a unique advantage by isolating motor speed from the primary model. With these controllers, motor speed becomes accessible and seamlessly integrated into the system. As a result, the control system for DSSEM drives utilizing such controllers typically includes both current and speed controllers. In this setup, the speed controller facilitates the injection of desired current into the current controller. It accomplishes this by monitoring the actual motor speed and calculating the variance between it and the reference speed. Detection of rotational speed commonly involves sensing the rotor position and converting it into speed ($\omega=d\theta/dt$). Importantly, the current controller operates independently of the model and does not necessitate speed information for its functioning. This characteristic enhances the robustness and adaptability of the DSSEM drive control system.

The preceding section presented the robust H_∞ tracking controller with the PI approach to address the tracking GARE and guarantee that the DSSEM drive's output speed can response to any speed changing without tuning process. For DSSEM, the suggested controller was only useful if the inductance profile was linear. Nonetheless, there was a significant nonlinearity in the DSSEM's inductance curve concerning rotor angle and current. The reluctances of DSSEMs varied in response to variations in the magnetic flux as the rotor rotated. The inductance profile for each phase reflected these modifications. Controlling DSSEM thus required both an adaptive estimation strategy for dynamic model parameters and an approach to characterize these fluctuations. A local linearization-based gain scheduling strategy was integrated with the H_∞ algorithm to enable the training in a locally linearized region via the H_∞ matrix, hence enabling the implementation of the H_∞ tracking algorithm for DSSEM and its nonlinear inductance profile. Benefits of gain scheduling included quick switching of H_∞ controllers through operating conditions, and less computing power requirement than other nonlinear adaptive dynamic control techniques like neural networks, which require highly sophisticated operations for real-world implementation. Availability of enough memory was necessary to register the learned H_∞ matrices in the lookup table entities, which was crucial for employing gain scheduling. The online training approach for the local H_∞ matrix and the structure of the H_∞ lookup table method is described in the following subsections. In the pursuit of expedited response times while mitigating the necessity for extensive training procedures, this methodology underscores the imperative inclusion of speed as an intrinsic component within the nonlinear system framework. Despite the ostensibly linear nature of the model with regard to speed, it is paramount to acknowledge the inherent involvement of speed within the system's structural framework. Consequently, the utilization of a two-dimensional H-array necessitates the continual adaptation and retraining of local H-nodes to effectively accommodate the dynamic variations in motor speed. While a two-dimensional array offers the advantage of reduced memory overhead compared to its three-dimensional counterpart, which integrates speed as an additional axis, it is imperative to recognize the potential trade-offs inherent in such an approach. Nonetheless, the proposed adoption of a three-dimensional table, as explicated in this study, holds significant promise in yielding markedly improved dynamics and responsiveness. By incorporating speed as a pivotal determinant within the model, this comprehensive approach not only facilitates a more nuanced comprehension of the system's behavioral dynamics but also engenders enhanced performance and adaptability. Thus, it represents a seminal advancement towards augmenting the efficacy and robustness of motor control systems in practical contexts.

A. The configuration of the mapping metrics protocol

An effective and simple method to illustrate the nonlinear surface of the inductance profile was to use a lookup table in conjunction with the mapping strategy. Different lookup table implementations, including torque [34], flux linkage, and inductance profile [35], were employed for DSSEM control. The H_∞ lookup table algorithm comprised three steps: packing, extraction, and interpolation. The packing procedure, which separated the inductance profile's surface into a sufficient number of H_∞ cores, was the first stage. Next, a sample of rotor angles and currents was chosen to create a bidirectional lookup table large enough to overcome the DSSEM's nonlinear

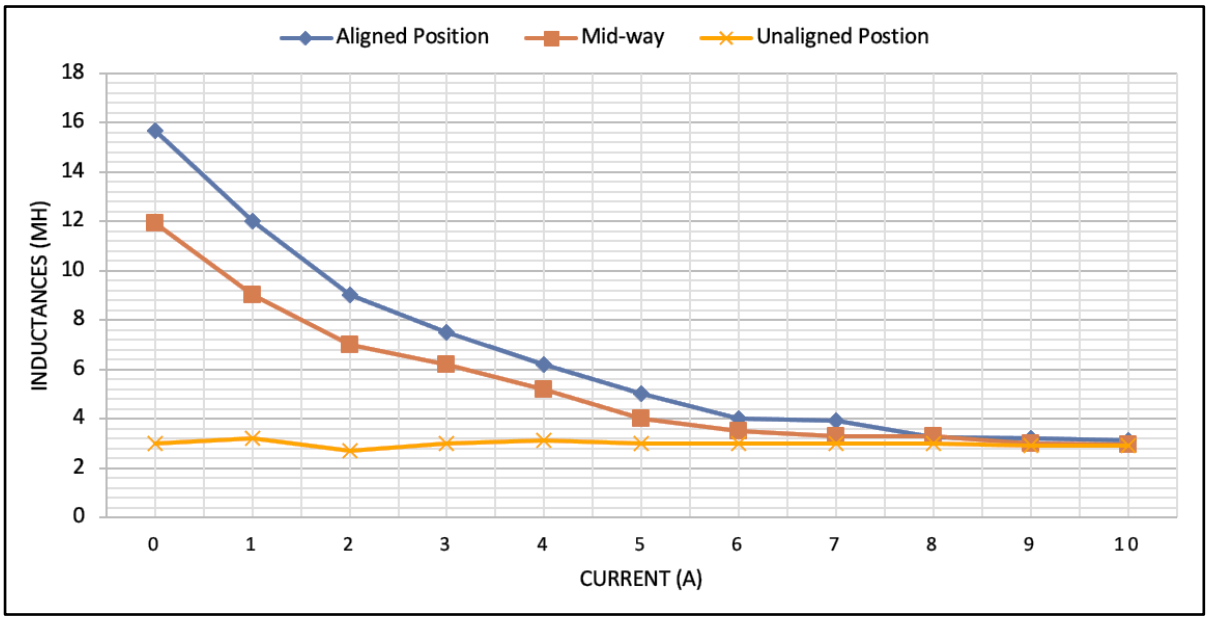

Fig 1. The nonlinear inductance profile of DSSEM.

domain. Each H∞ core was a local linear controller that can apply and learn linear equations. In order to train the H_∞ matrix until optimal values were achieved using the data observed in each preset segment, H_∞ tracking control was applied to each section. Each section's training H_∞ matrices was crammed into the table to create an array that held the H_∞ matrix. The extraction process, which took place in the second step, located the current trajectory in the table and extracted the H_∞ matrices that were closest to the current. Finding the single H_∞ matrix that aligned most closely with the present path was done by measuring the distances between the current and neighboring matrices. While this method aided the problem's resolution, its imprecise conclusions resulted in a disordered current route between the two cycles. In order to solve this problem, the third step used linear interpolation, which was a far more effective method than trying to locate the closest H_∞ matrix method for improving accuracy and outcomes through a smoother transition. This method estimated the new interpolated matrix at the current path by taking the distance-weighted average of the eight closest H_∞ matrices. This procedure suggested that the parameters of the estimated matrix were equally averaged based on equal distances if the estimated point was at the center of the closest predefined H_∞ matrix. To develop a speed controller capable of seamlessly adapting mechanical speed without requiring a reset of the learning process, it is essential to incorporate speed as a supplementary axis within the system's inductance surface. In order to achieve a fluid transition across the surface of the quantized 3D domain, it is crucial to introduce a sophisticated 3D interpolation mechanism into the existing table structure. This enhancement will enable the system to smoothly navigate through the multidimensional space, ensuring that the controller's responses remain consistent and accurate across varying operating conditions. The mapping function plays a pivotal role in this process, as it dictates how the interpolated H_∞ matrix is derived from the data stored within the 3D table. Defining this Algorithm can optimize the interpolation process to effectively capture the nuances of the system's behavior and ensure that the controller's speed actions align with the desired performance objectives. The mapping function for generating the mapped matrix can be expressed as:

$$H_s = H^T \forall^T \emptyset \tag{19}$$

$$H = [H_1 \quad H_2 \quad H_3 \quad H_4 \quad H_5 \quad H_6 \quad H_7 \quad H_8]$$

$$\forall = \begin{bmatrix} 1 & 0 & 0 & 0 & 0 & 0 & 0 & 0 \\ -1 & 0 & 0 & 0 & 1 & 0 & 0 & 0 \\ -1 & 0 & 1 & 0 & 0 & 0 & 0 & 0 \\ -1 & 1 & 0 & 0 & 0 & 0 & 0 & 0 \\ 1 & 0 & -1 & 0 & -1 & 0 & 1 & 0 \\ 1 & -1 & -1 & 1 & 0 & 0 & 0 & 0 \\ 1 & -1 & 0 & 0 & -1 & 1 & 0 & 0 \\ -1 & 1 & 1 & -1 & 1 & -1 & -1 & 1 \end{bmatrix}$$

$$\emptyset = [1 \quad \Delta i \quad \Delta\theta \quad \Delta\omega \quad \Delta i\Delta\theta \quad \Delta\theta\Delta\omega \quad \Delta\omega\Delta i \quad \Delta i\Delta\theta \; \Delta\omega]$$

where H is the eight nearest H-matrices to the H_s, $\forall$ is a predefined constant matrix, and $\emptyset$ is the vector of distances related to the three axises, and $\Delta i = (i - i_0/i_1 - i_0)$, $\Delta\theta = (\theta - \theta_0/\theta_1 - \theta_0)$, and $\Delta\omega = (\omega - \omega_0/\omega_1 - \omega_0)$. The parameters of 3D table scheduling are illustrated in Fig. 5.

B. Learning structure of the mapped matrices

This study employed least squares method to train and solve the H_∞ tracking problem by observing certain data sets, such as the cost function and system states, generated from the model during the machine trajectories. One of the main benefits of LS approaches was that they do not require additional models to determine model parameters. In practice, the control strategy was enhanced by including an observer to gather the states of the system states. The data packets received from system N were required to be at least $N \geq a(a+1)/2$ to meet the excitation requirement of the least square equations, where a denoted the total number of states. Also, It was necessary to perform the Kronecker product $\otimes$ to allow the user to build the cost function as linear in vectors (28). Then, $vec(P^{j+1})$ was created by compiling the columns of $the\ H_\infty$ matrix. Once enough time had elapsed to meet the persistence constraint, the batch LS equation was produced as follows:

$$vec(H^{j+1}) = (\Pi^T\Pi)^{-1}\Pi\mathcal{B} \tag{20}$$

$$\Pi = \left[(X_\Delta^k)^T \quad (X_\Delta^{k+1})^T \cdots (X_\Delta^{k+z-1})^T\right]$$

$$X_\Delta^k = X_{k+z}\otimes X_{k+z} - \gamma X_{k+z+1}\otimes X_{k+z+1}$$

$$\mathcal{B} = [h(X_k, u_k, w_k)^T \quad h(X_{k+1}, u_{k+1}, w_{k+1})^T \cdots h(X_{k+z}, u_{k+z}, w_{k+z})^T]$$

Policy iteration-based adaptive optimal control strategies rely on a persistent excitation condition (PE) to ensure thorough exploration of the state space. However, when the state nearly reaches the desired position and stabilizes, the persistent excitation condition may no longer hold. To mitigate this issue, an exploratory signal containing sinusoids of varying frequencies can be introduced into the control input to qualitatively maintain the persistence of excitation [29].

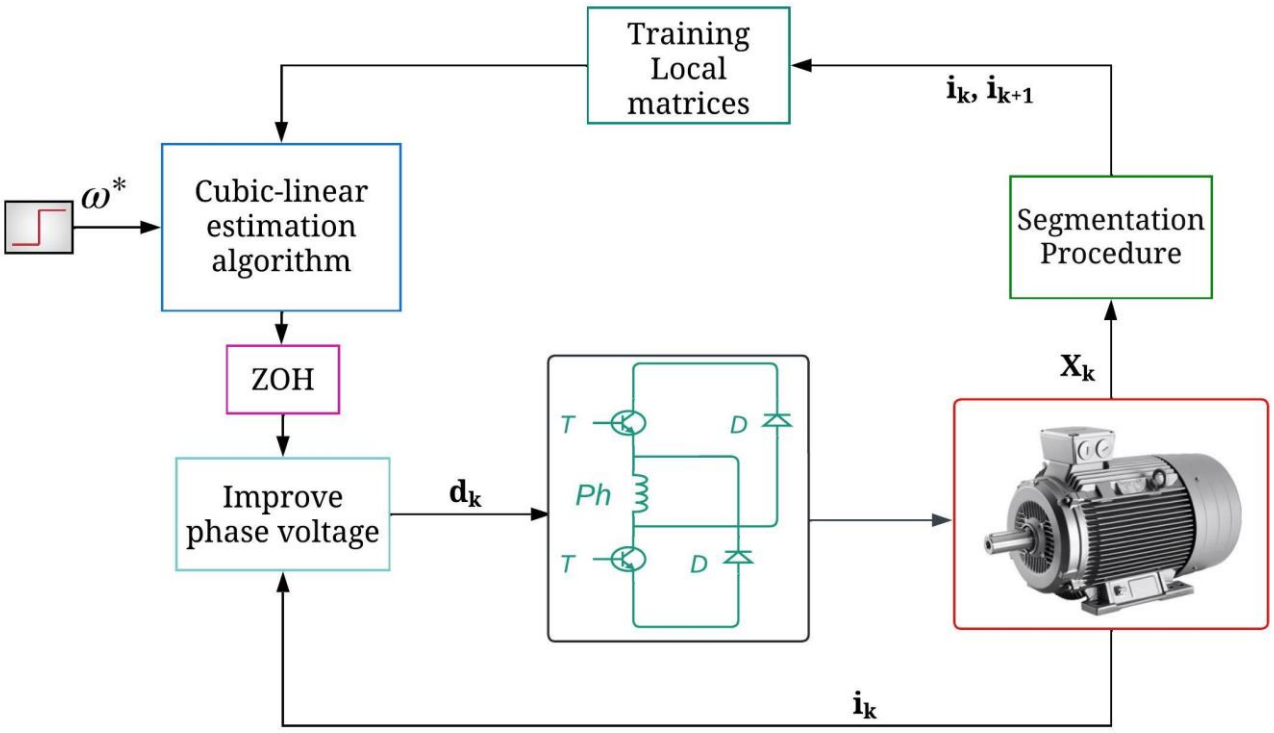

Fig 3. The block diagram of the proposed learning control.

IV. SIMULATION RESULTS

This section describes the execution and analysis of a simulation of the H_∞ tracking control using a linear interpolation approach to control the DSSEM drive's current. The most effective tool for designing the suggested scheme was MATLAB Simulink. The blocks for the simulation were constructed and adjusted using the 500 W DSSEM parameters that were examined in the experimental result. Fig 3 displays the suggested control blocks diagram. The motor had 12 poles on the stator and 8 poles in the rotor. It was a 3-phase motor with 2 Ω resistance for each phase and a nominal current of 5A. The motor had a maximum inductance of 16.6 mH and a minimum inductance of 6 mH. A range of 2.5-step rotor angles and 2-step sequence current values were registered to create a two-dimensional H_∞ core table. 100V was chosen as the available DC-link voltage. Based on the suggested controller's (10KHz) sampling frequency, a simulation step time of 100 microseconds was chosen. In order to enable the algorithm to train every local training centers that had been pre-specified on the nonlinear domain of the system, the tuning process was initiated with an acceptable control input and an augmented state, which were defined as $X_0 = [1 \quad 1]^T$ and $K_0 = [80 \quad -80]^T$, respectively. The least squares approach was used to train the local H_∞ matrix using 10 data tubules per iteration. In order to evaluate the suggested controller, the simulation operated under the assumption that the motor speed was initially at 60 RPM. Fig 4 shows that the local matrices has been fully learned after around 0.2 seconds of training. In this Fig, the rotational speed of shaft has been shifted up from 60 to 100 RPM. Fig 5 demonstrates the control that were applied to the motor during the training stage to meet the tracking performance requirements. Fig 6 illustrate the behavior of the disturbance input during the normal operating region. In this experimental setup, we utilized a sophisticated tridimensional table to facilitate comprehensive analysis. When we modified the rotational speed range from 60 to 100RPM, the speed response exhibited remarkable agility and stability throughout the duration of the training process. he concurrent variation in current corresponding to these alterations in motor speed meticulously provides valuable insights into the system's dynamic behavior. An intriguing observation arises when the speed changes at the 0.6-second mark: the local points remain unaffected and do not necessitate retraining. This phenomenon can be attributed to the incorporation of the speed axis within the learning centers. Consequently, even after initializing the algorithm and allowing the matrices to adapt to the plant, the controller seamlessly transitions to utilizing the plane corresponding to the measured speed. This seamless integration eliminates the need for re-adaptation, ensuring optimal utilization of optimal policy control regardless of the speed variation. This comprehensive analysis not only enhances our understanding of the system's behavior but also underscores the efficacy of the implemented control strategy in achieving stable and responsive performance across varying operating conditions.

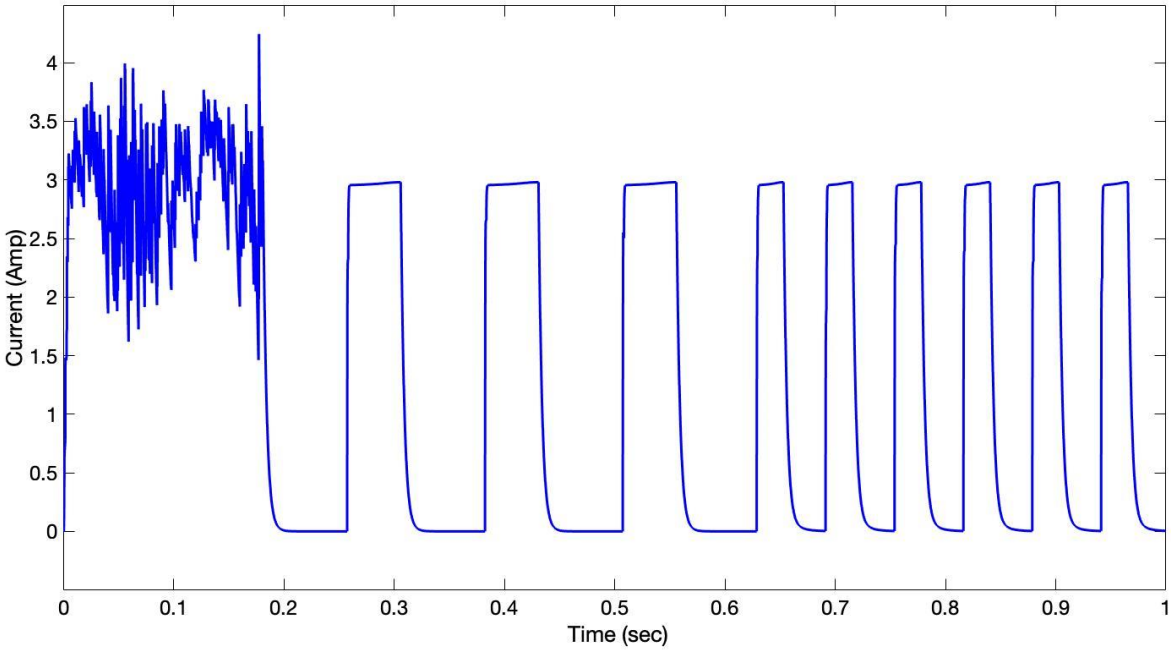

Fig 4. the behavior of the current waveform when the speed changed.

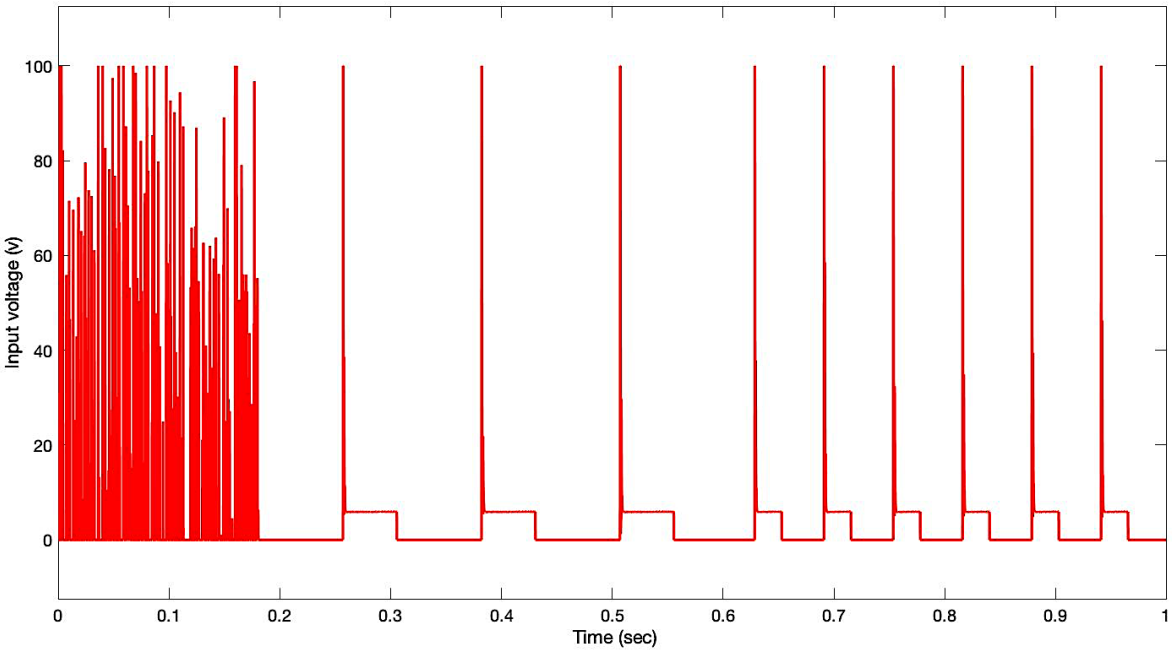

Fig 5. The input voltage during the training and normal operating condition.

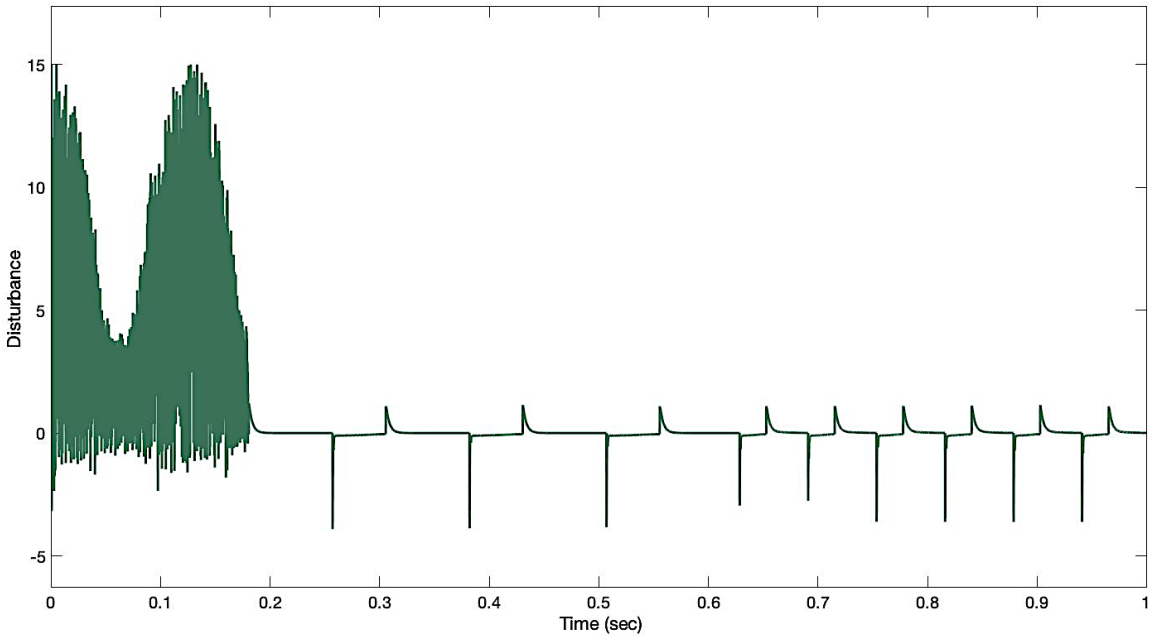

Fig 6. The behavior of the disturbances introduced to the system.

V. CONCLUSIONS

This work has researched a reinforcement robust H_∞ learning controller for regulating the speed of DSSEM. In addition to the zero-sum game problem, the H_∞ tracking control for the local linear region was examined and formulated. A lookup table was employed to illustrate the nonlinear inductance profile of motor. This lookup table was used to develop a mapping strategy for the proposed control scheme, which extended the linear controller to run in the nonlinear domain of system. The H_∞ centers located on the system's state trajectory were then tuned and mapped using an online training methodology. Cubic-linear estimation algorithm was employed to accomplish smooth variation of speed without requiring learning process. Lastly, the simulation findings were used to test the proposed speed control of DSSEM, demonstrating that the controller was robust and efficient in controlling the DSSEM speed. Moreover, there was a significant reduction in ripples along with a decrease in the effects of system disturbances.

ACKNOWLEDGMENT

The Researchers would like to thank the Deanship of Graduate Studies and Scientific Research at Qassim University for financial support (QU-APC-2024-9/1)

REFERENCES

[1] Sundaramoorthy, P.; Arun, V.; Mahadevan, B.; Venkatesh, P.; Reddy, P.V.A.; Mohan, S.S.; Reddy, S.R.K.; Reddy, S.S.K. Finite Element Analysis on Doubly Salient Singly Excited Machine for Electrified Transportation Systems. Prog. Electromagn. Res. C 2023, 135, 145–156.

[2] Wiguna, C.; Furqani, J.; Chiba, A. Improved Current Profile Selection for Noise Reduction of Switched Reluctance Motor at Middle Speed Considering Back EMF. IEEE Trans Ind Appl 2021, 57, 4707–4719, doi:10.1109/TIA.2021.3091085.

[3] Sun, X.; Wan, B.; Lei, G.; Tian, X.; Guo, Y.; Zhu, J. Multiobjective and Multiphysics Design Optimization of a Switched Reluctance Motor for Electric Vehicle Applications. IEEE Transactions on Energy Conversion 2021, 36, 3294–3304.

[4] Kimpara, M.L.M.; Reis, R.R.C.; Da Silva, L.E.B.; Pinto, J.O.P.; Fahimi, B. A Two-Step Control Approach for Torque Ripple and Vibration Reduction in Switched Reluctance Motor Drives. IEEE Access 2022, 10, 82106–82118, doi:10.1109/ACCESS.2022.3195493.

[5] Kawa, M.; Kiyota, K.; Furqani, J.; Chiba, A. Acoustic Noise Reduction of a High-Efficiency Switched Reluctance Motor for Hybrid Electric Vehicles with Novel Current Waveform. IEEE Trans Ind Appl 2018, 55, 2519–2528.

[6] Ling, X.; Li, B.; Gong, L.; Huang, Y.; Liu, C. Simulation of Switched Reluctance Motor Drive System Based on Multi-Physics Modeling Method. IEEE Access 2017, 5, 26184–26189, doi:10.1109/ACCESS.2017.2775340.

[7] Yan, N.; Cao, X.; Deng, Z. Direct Torque Control for Switched Reluctance Motor to Obtain High Torque–Ampere Ratio. IEEE Transactions on Industrial Electronics 2019, 66, 5144–5152, doi:10.1109/TIE.2018.2870355.

[8] Mehta, S.; Pramod, P.; Husain, I. Analysis of Dynamic Current Control Techniques for Switched Reluctance Motor Drives for High Performance Applications. In Proceedings of the 2019 IEEE Transportation Electrification Conference and Expo (ITEC); IEEE, 2019; pp. 1–7.

[9] Ibrahim, M. Switched Reluctance Motor Drives Speed Control Using Optimized PID Controller. PRZEGLĄD ELEKTROTECHNICZNY 2022, 1, 48–52, doi:10.15199/48.2022.11.07.

[10] Gobbi, R.; Ramar, K. Optimisation Techniques for a Hysteresis Current Controller to Minimise Torque Ripple in Switched Reluctance Motors. IET Electr Power Appl 2009, 3, 453, doi:10.1049/iet-epa.2008.0191.

[11] Shao, B.; Emadi, A. A Digital PWM Control for Switched Reluctance Motor Drives. In Proceedings of the 2010 IEEE Vehicle Power and Propulsion Conference; IEEE, 2010; pp. 1–6.

[12] azazy, B.; Abdel-Kader, F.; alsherif, mohsen; abdelqawee, islam Improved PI-Controller Of Switched Reluctance Motor For Torque Ripple Minimization In Electric Vehicle Applications. Engineering Research Journal - Faculty of Engineering (Shoubra) 2023, 52, 171–178, doi:10.21608/erjsh.2022.171006.1104.

[13] Quraan, L. Al; Saleh, A.L.; Szamel, L. Indirect Instantaneous Torque Control for Switched Reluctance Motor Based on Improved Torque Sharing Function. IEEE Access 2024, 12, 11810–11821, doi:10.1109/ACCESS.2024.3355389.

[14] Scalcon, F.P.; Fang, G.; Vieira, R.P.; Grundling, H.A.; Emadi, A. Discrete-Time Super-Twisting Sliding Mode Current Controller With Fixed Switching Frequency for Switched Reluctance Motors. IEEE Trans Power Electron 2022, 37, 3321–3333, doi:10.1109/TPEL.2021.3116096.

[15] Buriakovskyi, S.; Maslii, A.; Tyshchenko, A. Synthesis of the Speed Controller of the Switched Reluctance Motor. In Systems, Decision and Control in Energy V; Springer, 2023; pp. 179–193.

[16] Matwankar, C.S.; Pramanick, S.; Singh, B. Position Sensorless Torque Ripple Control of Switched Reluctance Motor Drive Using B-Spline Neural Network. In Proceedings of the IECON 2021 – 47th Annual Conference of the IEEE Industrial Electronics Society; IEEE, October 13 2021; pp. 1–6.

[17] Ahmad, S.S.; Thirumalasetty, M.; Narayanan, G. Predictive Current Control of Switched Reluctance Machine for Accurate Current Tracking to Enhance Torque Performance. IEEE Trans Ind Appl 2024, 60, 1837–1848, doi:10.1109/TIA.2023.3325306.

[18] Valencia, D.F.; Tarvirdilu-Asl, R.; Garcia, C.; Rodriguez, J.; Emadi, A. A Review of Predictive Control Techniques for Switched Reluctance Machine Drives. Part I: Fundamentals and Current Control. IEEE Transactions on Energy Conversion 2021, 36, 1313–1322, doi:10.1109/TEC.2020.3047983.

[19] Dyanamina, G.; Kakodia, S.K. Adaptive Neuro Fuzzy Inference System Based Decoupled Control for Neutral Point Clamped Multi Level Inverter Fed Induction Motor Drive. Chinese Journal of Electrical Engineering 2021, 7, 70–82, doi:10.23919/CJEE.2021.000017.

[20] Silva, W.A.; dos Reis, L.L.N.; Torrrico, B.C.; de C. Almeida, R.N. Speed Control in Switched Reluctance Motor Based on Generalized Predictive Control. In Proceedings of the 2013 Brazilian Power Electronics Conference; IEEE, October 2013; pp. 903–908.

[21] Alharkan, H.; Saadatmand, S.; Ferdowsi, M.; Shamsi, P. Speed Change Response of Switched Reluctance Motor Drives Under a Scheduled Q-Learning Scheme. In Proceedings of the 2020 52nd North American Power Symposium (NAPS); IEEE, April 11 2021; pp. 1–6.

[22] Alharkan, H. Torque Ripple Minimization of Variable Reluctance Motor Using Reinforcement Dual NNs Learning Architecture. Energies (Basel) 2023, 16, 4839, doi:10.3390/en16134839.
[23] Al-Tamimi, A.; Abu-Khalaf, M.; Lewis, F.L. Adaptive Critic Designs for Discrete-Time Zero-Sum Games with Application to H∞ Control. IEEE Transactions on Systems, Man, and Cybernetics, Part B: Cybernetics 2007, 37, 240–247, doi:10.1109/TSMCB.2006.880135.
[24] Yang, K.; Tang, X.; Qin, Y.; Huang, Y.; Wang, H.; Pu, H. Comparative Study of Trajectory Tracking Control for Automated Vehicles via Model Predictive Control and Robust H-Infinity State Feedback Control. Chinese Journal of Mechanical Engineering 2021, 34, 74, doi:10.1186/s10033-021-00590-3.
[25] Hu, C.; Jing, H.; Wang, R.; Yan, F.; Chadli, M. Robust H∞ Output-Feedback Control for Path Following of Autonomous Ground Vehicles. Mech Syst Signal Process 2016, 70, 414–427.
[26] Kiumarsi, B.; Lewis, F.L.; Jiang, Z.P. H∞ Control of Linear Discrete-Time Systems: Off-Policy Reinforcement Learning. Automatica 2017, 78, 144–152, doi:10.1016/j.automatica.2016.12.009.
[27] Li, X.; Xi, L.; Zha, W.; Peng, Z. Minimax Q-Learning Design for H∞ Control of Linear Discrete-Time Systems. Frontiers of Information Technology & Electronic Engineering 2022, 23, 438–451, doi:10.1631/FITEE.2000446.
[28] Aalipour, A.; Khani, A. Efficient and Real-Time Reinforcement Learning for Linear Quadratic Systems with Application to H-Infinity Control. In Proceedings of the 2023 62nd IEEE Conference on Decision and Control (CDC); IEEE, December 13 2023; pp. 6277–6282.
[29] Werbos, P.J.; Miller, W.T.; Sutton, R.S. A Menu of Designs for Reinforcement Learning over Time. Neural networks for control 1990, 67–95.
[30] Bertsekas, D. Multiagent Value Iteration Algorithms in Dynamic Programming and Reinforcement Learning. Results in Control and Optimization 2020, 1, 100003, doi:10.1016/j.rico.2020.100003.
[31] He, W.; Gao, H.; Zhou, C.; Yang, C.; Li, Z. Reinforcement Learning Control of a Flexible Two-Link Manipulator: An Experimental Investigation. IEEE Trans Syst Man Cybern Syst 2021, 51, 7326–7336, doi:10.1109/TSMC.2020.2975232.
[32] Yang, Y.; Wan, Y.; Zhu, J.; Lewis, F.L. H ∞ Tracking Control for Linear Discrete-Time Systems: Model-Free Q-Learning Designs. IEEE Control Syst Lett 2021, 5, 175–180, doi:10.1109/LCSYS.2020.3001241.
[33] Liu, Y.; Wang, Z.; Shi, Z. H∞ Tracking Control for Linear Discrete-time Systems via Reinforcement Learning. International Journal of Robust and Nonlinear Control 2020, 30, 282–301.
[34] Wei, Z.; Zhao, M.; Liu, X.; Lu, M. Speed Control for SRM Drive System Based on Switching Variable Proportional Desaturation PI Regulator. IEEE Access 2021, 9, 69735–69746, doi:10.1109/ACCESS.2021.3078194.
[35] Kotb, H.; Yakout, A.H.; Attia, M.A.; Turky, R.A.; AboRas, K.M. Speed Control and Torque Ripple Minimization of SRM Using Local Unimodal Sampling and Spotted Hyena Algorithms Based Cascaded PID Controller. Ain Shams Engineering Journal 2022, 13, 101719, doi:10.1016/j.asej.2022.101719.